Ann. Geophys., 31, 1507–1520, 2013
www.ann-geophys.net/31/1507/2013/
doi:10.5194/angeo-31-1507-2013

Annales Geophysicae
Open Access

Global characteristics of Pc1 magnetic pulsations during solar cycle 23 deduced from CHAMP data

J. Park, H. Lühr, and J. Rauberg

GFZ, German Research Center for Geosciences, Potsdam, Germany

Correspondence to: J. Park (park@gfz-potsdam.de)

Received: 3 July 2013 – Revised: 30 July 2013 – Accepted: 30 July 2013 – Published: 5 September 2013

Abstract. We present a global climatology of Pc1 pulsations as observed by the CHAMP satellite from 2000 to 2010. The Pc1 center frequency and bandwidth are about 1 and 0.5 Hz, respectively. The ellipticity is mostly linear with the major axis almost aligned with the magnetic zonal direction. The diurnal variation of Pc1 occurrences shows a primary maximum early in the morning and a secondary maximum during pre-midnight hours. The annual variations of the occurrence rates exhibit a clear preference for local summer. The solar cycle dependence of the occurrence rate reveals a maximum at the declining phase (2004–2005). Neither magnetic activity nor solar wind velocity controls the Pc1 occurrence rate significantly. Pc1 occurrence rate peaks at subauroral latitudes, but the steep cutoff towards higher latitudes is due to auroral field-aligned currents masking the Pc1 pulsations. The center frequency of Pc1 pulsations does not show a clear dependence on latitude. The global distribution of Pc1 exhibits highest occurrence rates near the longitude sector of the South Atlantic Anomaly. Pc1 events at auroral latitudes, although they are rarely detected, show a clear occurrence peak around local noon. A majority of the auroral Pc1 events are observed during solar minimum years.

Keywords. Magnetospheric physics (plasma waves and instabilities)

1 Introduction

Pc1 pulsations are geomagnetic fluctuations in the frequency range between 0.2 to 5 Hz. The geophysical importance of Pc1 pulsations consists in their close connection to (1) subauroral proton aurora with proton precipitation (e.g. Sakaguchi et al., 2008; Yahnin et al., 2009), (2) rapid dropout of relativistic electrons from the radiation belt (e.g. Miyoshi et al., 2008), and (3) traveling convection vortices (Engebretson et al., 2013). The pulsations are observed under a wide variety of geomagnetic field configurations. They frequently occur in the subauroral region (e.g. Fraser et al., 1996; Nomura et al., 2012) and in the auroral region (e.g. Roldugin et al., 2013). However, Pc1 pulsations appear also in regions of open geomagnetic field lines, such as cusp/mantle (e.g. Engebretson et al., 2009, 2012) and in the polar cap (e.g. Safargaleev et al., 2004). They appear even on magnetosheath field lines that are not connected to the Earth (e.g. Anderson et al., 1991; Anderson and Fuselier, 1993). In this paper we focus on Pc1 pulsations occurring on closed geomagnetic fields.

Observationally, Pc1 pulsations on closed geomagnetic field lines have been investigated using high-altitude satellites (e.g. Anderson et al., 1992a,b, 1996; Posch et al., 2010; Min et al., 2012); mid-altitude satellites, e.g. Viking (e.g. Erlandson et al., 1990); low-Earth-orbit (LEO) satellites, e.g. the Magsat (e.g. Iyemori and Hayashi, 1989), the Dynamic Explorer-2 (DE-2) (e.g. Iyemori et al., 1994; Erlandson and Anderson, 1996), Freja (e.g. Bräysy et al., 1998), or Space Technology 5 (ST-5) (e.g. Engebretson et al., 2008); and ground-based observations (e.g. Kawamura et al., 1983; Mursula et al., 2001; Kim et al., 2011). The electromagnetic ion cyclotron (EMIC) instability at high altitudes is generally considered as the source of Pc1 pulsations. When propagating from the source regions to the ground the pulsations may experience a series of changes in their properties. For example, the polarization can change (1) due to a superposition of waves of different origins, or (2) when the pulsations pass a region where the frequency is the same as the cross-over frequency of heavy ions (Denton et al., 1996). At high-altitude in near-equatorial regions the wave normal of Pc1 pulsations can be either parallel or oblique to the geomagnetic field lines (Min et al., 2012). In the ionosphere, on the other hand, the

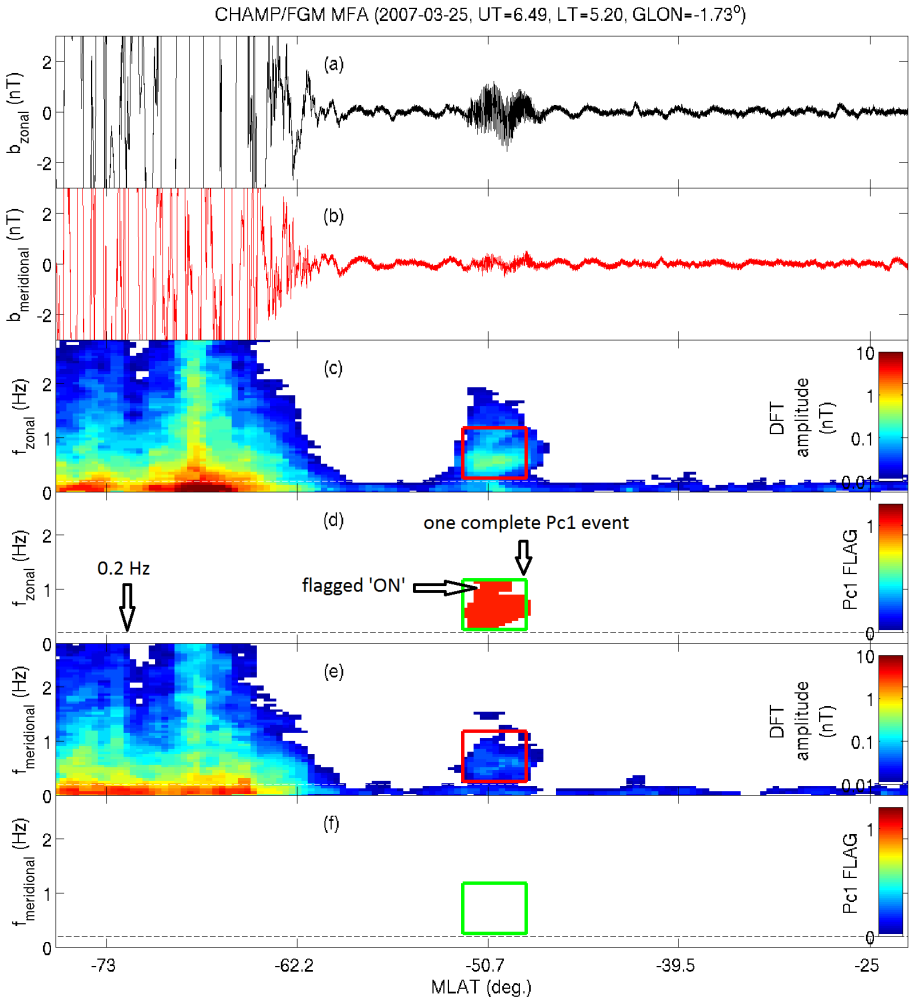

Fig. 1. An example of a Pc1 event detected automatically by our algorithm: **(a)** time series of 50 Hz zonal B-field variation, **(b)** meridional B-field variation, **(c)** dynamic spectrum of zonal B-field, **(d)** Pc1 detection flag in zonal B-field (red area), **(e)** spectrum of meridional B-field, **(f)** Pc1 detection flag of meridional B-field. The rectangles in panels **(c)**–**(f)** represent the frequency vs. time range of a detected Pc1 event. The horizontal dashed line at 0.2 Hz in panels **(d)** and **(f)** represents the lower frequency limit of the Pc1 range.

pulsations can be ducted across the magnetic field so that they are observed at locations, which are not conjugate to the high-altitude source region (Lysak and Yoshikawa, 2006). The Pc1 can also stimulate the ionospheric Alfvén resonator (IAR), and persist long if the pulsation frequency matches the IAR specific frequency (Lysak et al., 2013).

As a consequence of the features outlined in the previous paragraph, the climatology of Pc1 pulsations is expected to show differences between observations in near-equatorial/high-altitude regions, in the ionosphere, and on the ground. In the outer magnetosphere near the geomagnetic equator, Pc1 pulsations generally occur in the early-afternoon sector (Anderson et al., 1992a,b; Erlandson and Ukhorskiy, 2001; Halford et al., 2010; Clausen et al., 2011; Keika et al., 2013). They are dominantly transverse (Anderson et al., 1992a). The polarization is mostly linear in the dawn/morning sector and left-handed (LH) in the afternoon, while right-handed (RH) Pc1 pulsations are relatively rare (Anderson et al., 1992b, Fig. 1).

On the ground, the occurrence rate depends in a complex manner on magnetic latitude (MLAT) and magnetic local time (MLT). In Parkfield, California ($L \sim 1.8$), the occurrence rate is much higher at night than during daytime (Bortnik et al., 2007, Fig. 6). The occurrence rate peaks near dawn with a secondary noontime maximum at the station Uzur near Irkutsk ($L \sim 1.8$). At higher L shells the occurrence maximum shifts to later MLT sectors. For example, the occurrence rate at Eights Station in Antarctica ($L \sim 3.9$) peaks in a broad MLT range in the morning sector, and that of the Sodankylä observatory ($L \sim 5.1$) exhibits a clear peak near noon (see Kangas et al., 1998, and references therein).

The seasonal variation, according to a limited number of studies on this subject, also exhibits a dependence on latitude. Ground observations by Kuwashima et al. (1981)

demonstrated that Pc1 events prefer local winter (equinox) for mid-latitude (high-latitude) regions. Later, Nomura et al. (2011) confirmed that mid-latitude Pc1 events are more active in local winter than in summer. The solar cycle dependence also seems to vary with latitudes. In Sodankylä (Finland) the Pc1 occurrence rate appears inversely correlated with solar activity, and the phase delay between the two is less than 1 year (Mursula et al., 1991), which was explained in terms of magnetospheric ion composition (Guglielmi and Kangas, 2007, Fig. 3). On the other hand, Pc1 activity in California (USA) is strongest during the declining phase of a solar cycle (Fraser-Smith, 1970, and references therein).

The polarization of Pc1 pulsations on the ground can be either linear, LH, or RH. At mid-latitudes the polarization obviously depends on frequency (Nomura et al., 2011), and the major axis of the polarization ellipse points to the source location when the observation point is far from the source (Nomura et al., 2012).

There have been only a few papers on Pc1 observations at LEO. Iyemori and Hayashi (1989) analyzed five Pc1 events observed by Magsat on the duskside. LH and RH polarizations coexisted for the events, and the spatial scale size was about 40–80 km. Iyemori et al. (1994) reported statistics of "large-amplitude" Pc1 pulsations using the DE-2 satellite. A majority of the events occurred in the afternoon, and Pc1 pulsations did not necessarily accompany electron temperature enhancements. Erlandson and Anderson (1996) also examined the DE-2 data, and found no altitude dependence of the Pc1 occurrence rate. Most of the Pc1 events occurred near dawn (04:00–06:00 MLT) or noon (10:00–15:00 MLT). Engebretson et al. (2008) investigated the Pc1 climatology using the ST-5 satellite. The Pc1 occurrence rate in that paper was higher for storm recovery phase than during other phases of storms. For further details on Pc1 pulsations readers are referred to the reviews by Guglielmi and Pokhotelov (1996), Kangas et al. (1998) or Mursula (2007).

The ionosphere is quite important for Pc1 studies in that it hosts conversion and coupling of different Pc1 modes, bridging the gap between magnetospheric and ground-based observations of Pc1 pulsations. Although previous studies using LEO satellites have given us general ideas on ionospheric Pc1, there are still open issues. First, the local time (LT) of Magsat or ST-5 was fixed (dawn/dusk), and in the case of DE-2 the LT cannot be decoupled from seasonal variations (e.g. Saito et al., 1995). Second, none of the previous Pc1 observations by LEO satellites spanned a full solar cycle. Third, little has been published about the geographic distribution of Pc1 occurrence rates. In this study we investigate the Pc1 climatology in the ionospheric F region using a globally homogeneous survey by the CHAllenging Minisatellite Payload (CHAMP) satellite, which covered 10 years from July 2000 to September 2010. Section 2 is dedicated to describing satellite instruments and the automatic event detection method. In Sect. 3 we present the climatology of Pc1 pulsations. The results are discussed in Sect. 4, and conclusions are drawn in Sect. 5.

2 Instruments and event detection methods

2.1 Instrument and data

The CHAMP satellite was launched in July 2000 into a polar orbit with an inclination angle of about 87°. The initial altitude was about 450 km, which decreased slowly to 250 km at the time of atmospheric re-entry in September 2010. The orbit precessed slowly through LT. It took about 131 days to obtain a full LT coverage when considering both up- and down-leg parts. CHAMP carried a flux-gate magnetometer (FGM) measuring the geomagnetic field vectors at a rate of 50 Hz. The root-mean-square (RMS) noise level of FGM data is less than 0.05 nT. In this study we use the 50 Hz FGM data as recorded in the sensor coordinate system. To identify Pc1 pulsations we interpret magnetic field data in the mean-field-aligned (MFA) frame. MFA coordinates are defined as follows: the z component (hereafter "parallel" component) is along the mean field, the y component (hereafter "zonal" component) is perpendicular to the mean field and parallel to the ground (pointing eastward), and the x component (hereafter "meridional" component) completes the triad, pointing outward.

For the transformation into the MFA frame we do not use the traditional and rigorous approach, which starts from 1 Hz geomagnetic field data in north–east–center (NEC) coordinates and uses geomagnetic field models to define the "mean field" (see, for example, Park et al., 2009, for more details). We actually employ magnetic field readings in their sensor frame. This avoids attitude noise that is introduced by the uncertainty of the star tracker readings when transforming the fields into the NEC frame. In our case the mean field is deduced from the in situ field measurements that are low-pass filtered with a cut-off period of 60 s. From this smoothed ambient field we deduce the local declination and inclination, which are needed for the transformation from the sensor frame into the MFA frame. In this frame the two transverse components are usually small outside the auroral oval (see Figs. 1a–b). The z component comprises practically the total field strength.

As a next step we apply a discrete Fourier transform (DFT) to the zonal and meridional components with a moving window. The window size is 1024 data points (approximately 20 s long), returning a spectrum over 25 Hz with a frequency resolution of about 0.05 Hz. The DFT window is moved forward in 10 s steps, providing a signal overlap. As a result we get DFT dynamic spectra over all the years for the zonal and meridional components. An example is shown in Fig. 1, panels (c) and (e).

2.2 Event detection method

In order to detect Pc1 pulsations automatically the following procedure is applied to the dynamic spectra of the zonal (Fig. 1c) and meridional (Fig. 1e) components. First, the spectra are smoothed by a two-dimensional (3-by-3) median low-pass filter in order to eliminate stand-alone peaks. This filtering is used only for event detection but is not applied in the wave property analysis that is described in subsequent paragraphs. Note that Figs. 1c and 1e show filtered dynamic spectra.

To identify Pc1 events we check each DFT spectrum for the following conditions. According to Erlandson and Anderson (1996) fluctuations below 0.2 Hz (below the horizontal dashed lines in Figs. 1d and f) are caused by small-scale field-aligned currents (FACs) or by other types of pulsations. In case the spectral amplitudes (the absolute magnitude of the DFT results, in nT) below 0.2 Hz are larger than 1 nT, we consider the corresponding spectrum as dominated by FACs and neglect it. This method also helps to prevent contaminations by magnetic fluctuations originating from broad-band pulsations, equatorial plasma bubble (EPB) (e.g. Stolle et al., 2006) or from medium-scale traveling ionospheric disturbance (MSTID) (e.g. Park et al., 2009). Conversely, an inherent drawback of this method is the systematic exclusion of Pc1 events within the auroral oval due to their collocation with small-scale FAC structures (e.g. Rother et al., 2007).

As a second step of the EMIC detection procedure we search in all spectra for wave activities above 0.2 Hz. All the spectral bins in which the amplitude in this upper band is larger than 0.05 nT are flagged "ON". These flagged spectral bins are considered as candidates for Pc1 events. Finally, the third step requires that the wave activity above 0.2 Hz should be independent of the activity below 0.2 Hz. Hence, we search for the minimum spectral amplitude in the frequency range from 0.2 Hz down to the maximum amplitude frequency, and this minimum should be lower than a half of the maximum spectral amplitude above 0.2 Hz.

This procedure is repeated for all the spectra of a day separately for the two transverse components. We further apply our 3-by-3 low-pass median filter to all the ON-flagged spectral bins in order to remove solitary peaks. An identified Pc1 event is shown, as one example, in Figs. 1d and f as red patches. Then we combine the zonal and meridional ON-flagged spectral bins. The smallest rectangle in frequency vs. time space that encompasses all the adjacent ON-flagged bins in the zonal and meridional components is combined to one Pc1 event (see the rectangles in Figs. 1c–f). When the time gap between two ON areas is longer than 30 s, the subsequent ON region is considered as a separate Pc1 event. When the duration of an ON region is shorter than 30 s (200 km along-track), we disregard the event. For each Pc1 event the start/stop time, the highest/lowest frequency, geographic positions (geographic latitude (GLAT)/geographic longitude (GLON)), geomagnetic (MLAT/MLT) positions, and maximum spectral amplitude are recorded.

Further, we deduce the elliptical polarization parameters of each Pc1 event, i.e. degree of polarization, ellipticity, azimuth angle of the major axis (0°: zonal direction, 90°: meridional direction). Here we apply the methodology described in Fowler et al. (1967) and Bortnik et al. (2007) to the original dynamic spectra, which are not modified by the 3-by-3 median filter.

3 Climatology of Pc1 events

For this study we considered CHAMP/FGM magnetic field observations of the time from 19 July 2000 to 17 September 2010. The yearly averaged solar flux index, F10.7, decreased from 180 to 80 solar flux units (sfu). From the available observations our method of automatic Pc1 detection has found 3904 events in total. We exclude events with unreasonable properties by imposing the following criteria: (1) upper frequency should not exceed 5 Hz, (2) maximum spectral amplitude should not exceed 3 nT, and (3) Kp index should not exceed 6.3. In total 3616 events (1638/1978 events in the Northern/Southern Hemisphere) survived the exclusion conditions, and are investigated in the following subsections.

3.1 Properties of Pc1 pulsation

In this subsection we investigate general wave properties of the detected Pc1 events. Figure 2 presents histograms of the center frequency, bandwidth, and maximum spectral amplitude. The center frequency peaks around 1 Hz (0.5–1.5 Hz). The bandwidth is narrow so that a majority of events have a bandwidth less than 1 Hz. The maximum spectral amplitude is generally below 0.5 nT. Note that the maximum spectral amplitude in Fig. 2 is not the peak-to-peak amplitude of a Pc1 event, but the maximum spectral (DFT) amplitude among all the spectral bins belonging to a Pc1 event.

Figure 3 visualizes the polarization properties. Each black dot in the scatter plots corresponds to one Pc1 event, and the red lines represent annual median values (thick solid line with squares) and quartiles (thin dashed lines) of the respective polarization properties. Panel (a) shows the degree of polarization, which signifies the ratio of polarized power to the total power in the Pc1 frequency band. The polarization degree is quite high with the annual median ranging around 0.85 during almost all the years investigated. The ellipticity (0: linear, 1: circular) is very small in magnitude (annual median < 0.02), which means that the detected Pc1 events are linearly polarized. The azimuth angle in Fig. 3c is defined as the angle between the major axis of the polarization ellipse and the magnetic zonal (y) direction. For 0° the major axis is parallel to the magnetic east–west direction, while for $\pm 90°$ it is pointing outward–inward, normal to the L shell. The derived mean azimuth angle of the major axis

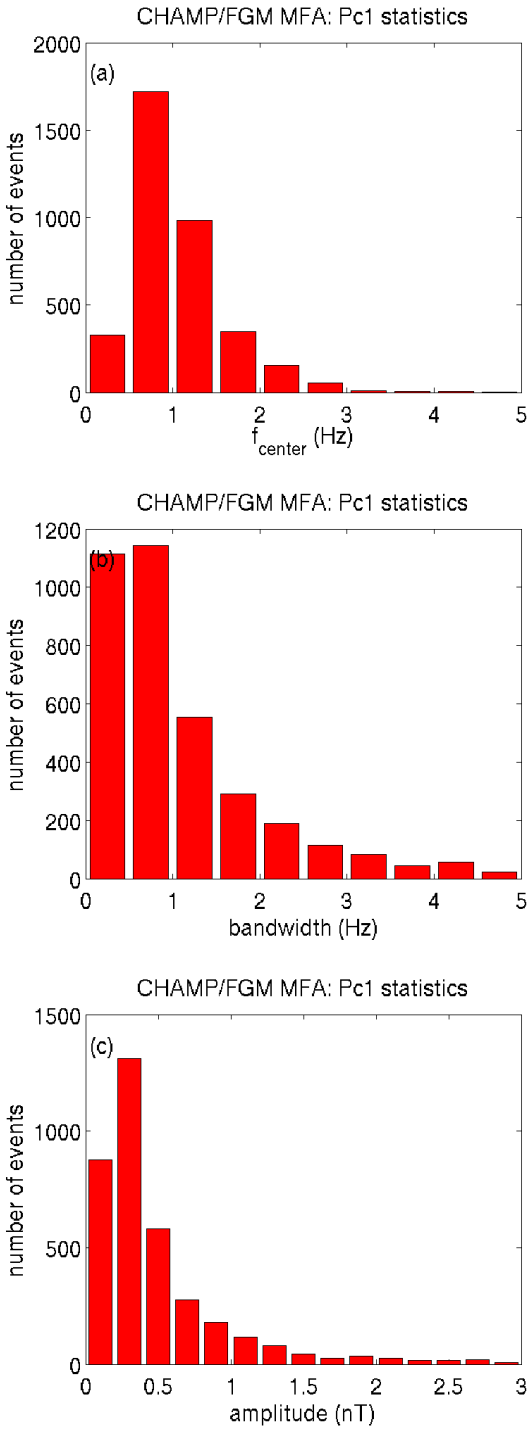

Fig. 2. Histograms of **(a)** center frequency, **(b)** bandwidth, and **(c)** maximum spectral amplitude of the Pc1 events detected by CHAMP/FGM.

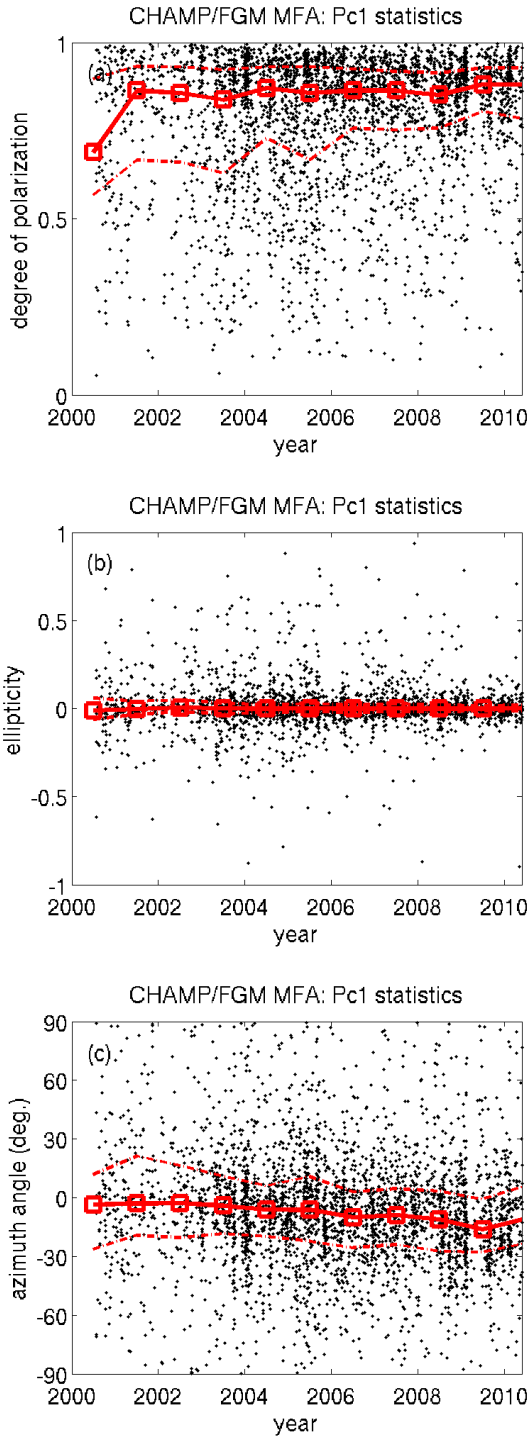

Fig. 3. Solar cycle variation of the Pc1 polarization properties: **(a)** degree of polarization, **(b)** ellipticity, **(c)** azimuth angle between the major axis and the zonal direction. The black dots show all the Pc1 events, and the red squares represent annual median values, with their range of quartiles shown as dashed lines.

is generally very small in magnitude, in particular during the early years. Around solar minimum it increases up to some $-10°$, which means that the major axis points westward/poleward and eastward/equatorward. There is no significant difference in polarization properties between the two hemispheres (figures not shown). All these results imply that

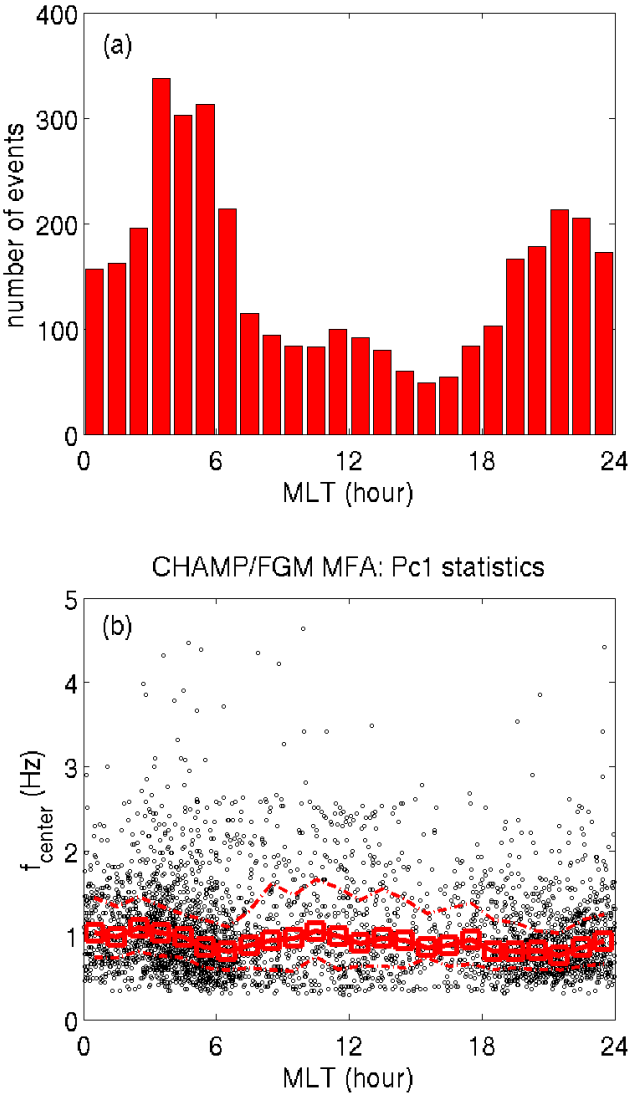

Fig. 4. Diurnal variation of **(a)** number of detected Pc1 events and **(b)** Pc1 center frequency. The black dots in **(b)** show all the Pc1 events, and the red squares represent median values with their range of quartiles shown as dashed lines.

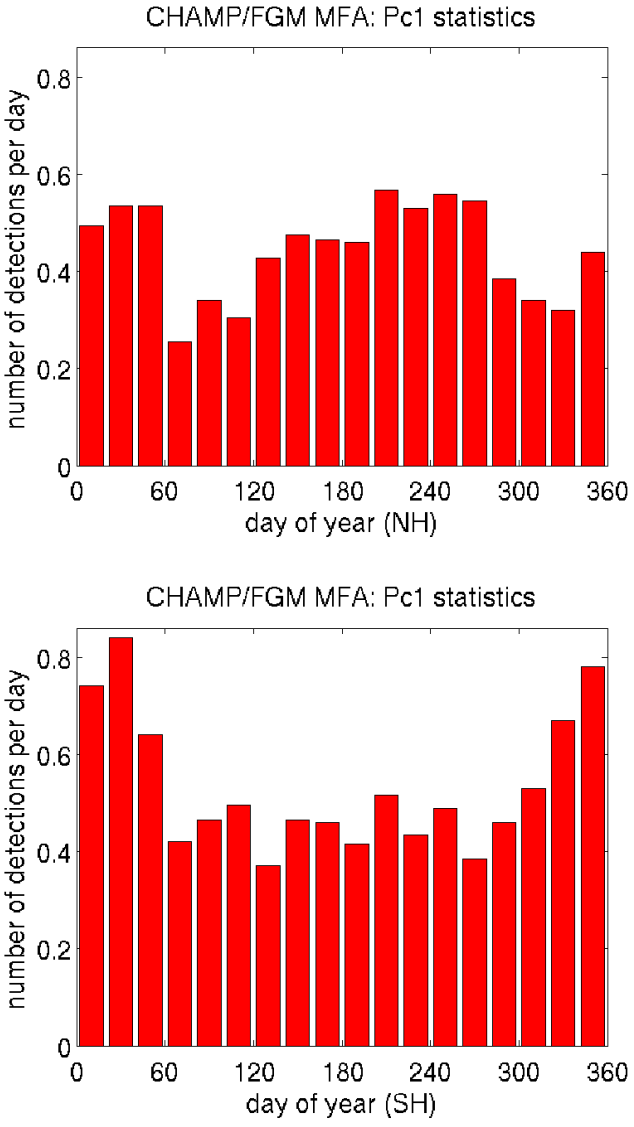

Fig. 5. Annual variation of Pc1 occurrence rates separately for **(a)** Northern and **(b)** Southern Hemisphere.

the detected Pc1 events are dominated by linearly polarized zonal magnetic fluctuations. The azimuth of oscillation rotates a little bit away from the zonal direction during solar minimum.

3.2 Temporal variation of event rates

In this subsection we first address the MLT dependence of Pc1 occurrences and of the center frequency. Figure 4a presents a histogram of the number of detected Pc1 events versus MLT hour. The Pc1 events occur preferentially at nighttime with the main peak around 04:00 MLT and a secondary maximum around 21:00 MLT. Dayside Pc1 occurrence is quite low, while there appears a small peak around 12:00 MLT. The dependence of the center frequency on MLT (Fig. 4b) exhibits no clear trend: it stays close to 1 Hz all day. Apparent diurnal frequency variations are considered to be smaller than the inter-quartile range.

Figure 5 shows the annual variation of the number of Pc1 events detected per day, separately for the two hemispheres (panel a for Northern and panel b for Southern Hemisphere). In both hemispheres the Pc1 occurrence is slightly enhanced around local summer compared to other times of the year (seasonal variation). Superimposed on that there seems to be a global annual cycle with the July minimum, which is well known for the ionospheric F2 layer (e.g. Rishbeth and Müller-Wodarg, 2006). In the Southern Hemisphere the two cycles (i.e. the seasonal and annual variations) seem to be approximately in phase, causing the large difference between

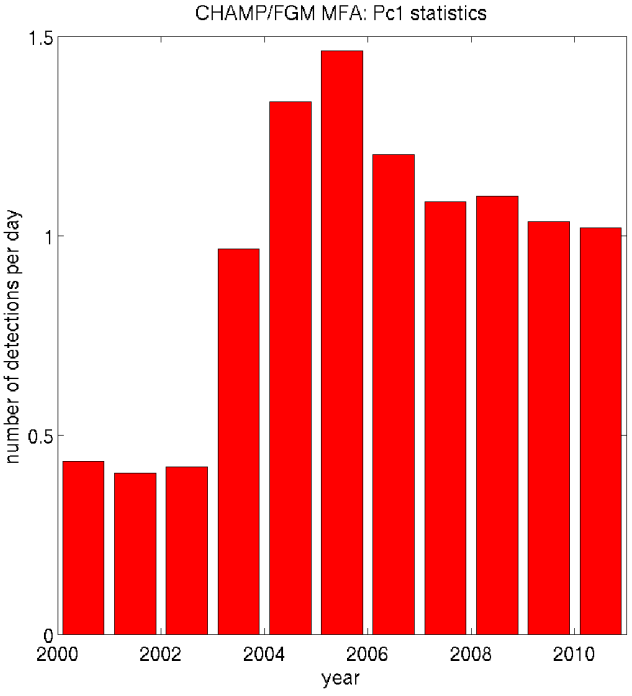

Fig. 6. Solar cycle variation of the Pc1 occurrence rate.

June and December solstices. The anti-phase of the two cycles in the Northern Hemisphere seems to largely reduce the difference between the solstices.

Figure 6 shows the solar cycle variation of the number of Pc1 events detected per day. The Pc1 occurrence rate is highest during 2005, when the solar activity was on the transition from maximum to minimum. The occurrence during solar minimum years (2007–2010) by far exceeds that of the solar maximum years (2000–2002). The center frequency of Pc1 events does not exhibit a clear dependence on solar activity (figure not shown).

3.3 Spatial distribution of occurrence rate

Here we are interested in how the characteristics of Pc1 events depend on latitude and longitude. Figure 7a shows the number of detected Pc1 events as a function of MLAT. In both hemispheres the occurrence rate peaks between 55 and 60° MLAT. In the Southern Hemisphere a significant number of events are found at latitudes higher than 65° MLAT. Figure 7b presents the center frequency as a function of magnetic latitude; black dots mark each Pc1 event, and the red squares represent median values at 5° MLAT intervals with their range of quartiles shown as dashed lines. Although the median in Fig. 7b exhibits a certain variation with latitude, we question its significance because of the considerable range of quartiles. Somewhat interesting are the events beyond 70° MLAT, of which the center frequencies are lower than at lower latitudes.

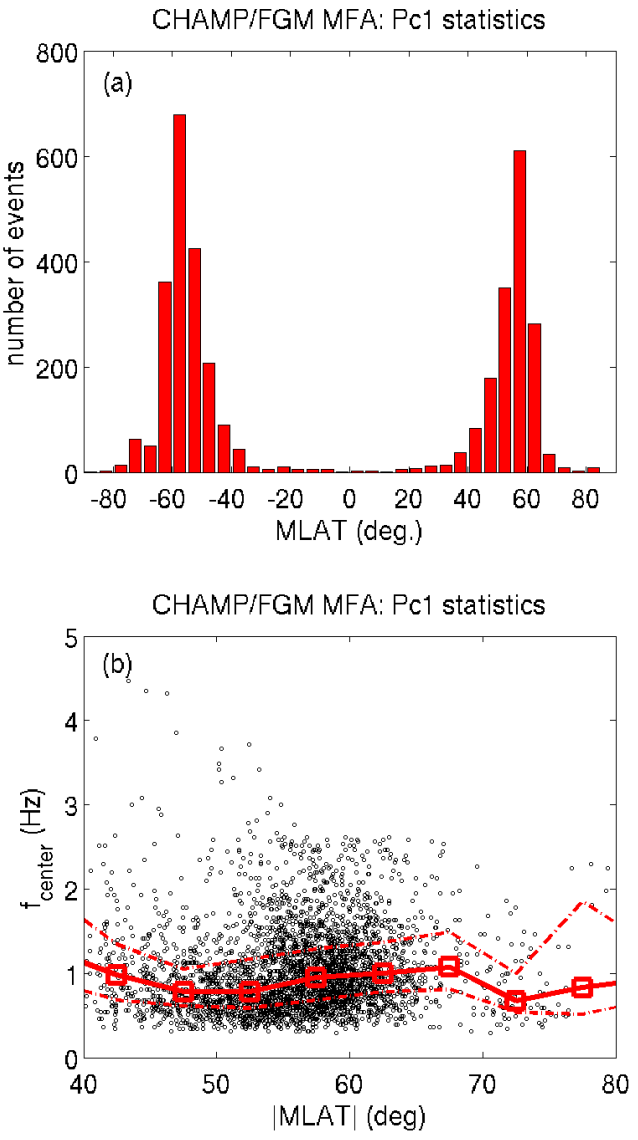

Fig. 7. Latitude dependence of **(a)** number of detected Pc1 events, and **(b)** Pc1 center frequency. The black dots in **(b)** show all the Pc1 events, and the red squares represent median values with their range of quartiles shown as dashed lines.

Figure 8 shows the geographic distribution of Pc1 events. Panel (a) presents a scatter plot of all the Pc1 events. The blue dashed curves represent MLAT contours at 30° intervals. The clear cutoff of events beyond 65° MLAT could be a consequence of the auroral oval with its intense FAC that masks the tiny signal of Pc1 events. However, as pointed out in the preceding paragraph, a significant number of Pc1 events exist in the southern hemispheric auroral oval: in particular in the sector around 60° W GLON, where MLAT lines reach highest GLAT. This group of events will be discussed further in Sect. 4.3.

Figure 8b presents the geographic distribution of Pc1 occurrence rates. The number of Pc1 detections within a bin of

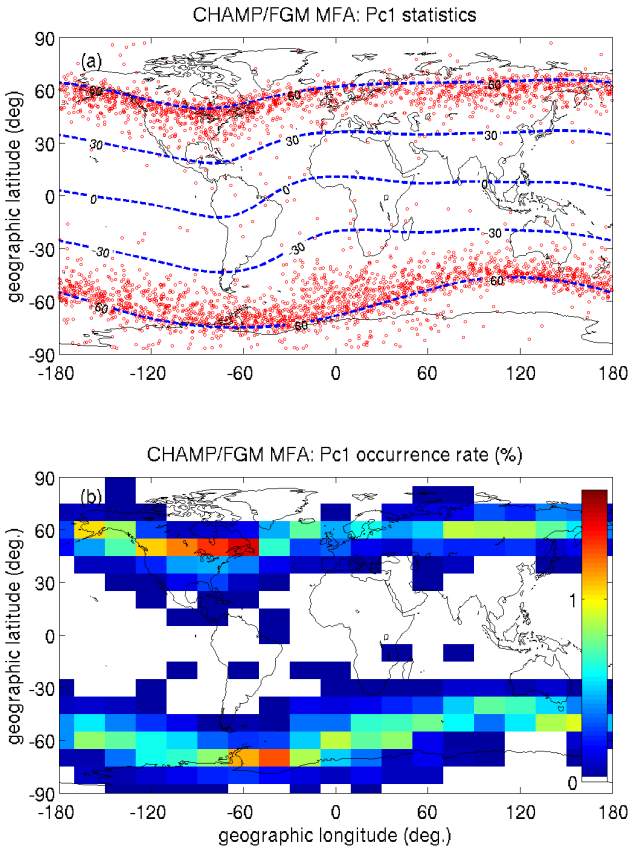

Fig. 8. Global distribution of the Pc1 events: **(a)** scatter plot of individual events, and **(b)** occurrence rate normalized by the number of CHAMP passes over that bin. The blue dashed curves in **(a)** represent MLAT contours at 30° intervals.

size 10° GLAT by 20° GLON is normalized by the number of CHAMP passes over that bin. During the mission CHAMP circled the Earth more than 58 000 times, which corresponds approximately to 6450 passes over each bin. Normalization with this constant value (6450) is applied uniformly to all the bins. High occurrence rates are observed equatorward of 60° MLAT, consistent with Fig. 7a. Of interest is the GLON dependence. In the Northern Hemisphere the Pc1 occurrence rates are high over North America, reaching up to 1.4 % over Newfoundland. In the Southern Hemisphere the occurrence rates maximize in the same GLON sector. The collocation of the active Pc1 region with the South Atlantic Anomaly (SAA) suggests that Pc1 event generation is favored by the low magnetic field in this region. When combining the GLON distribution with the Pc1 occurrence peak at 04:00 MLT, the highest event rates on a global scale are expected around 09:00 UT.

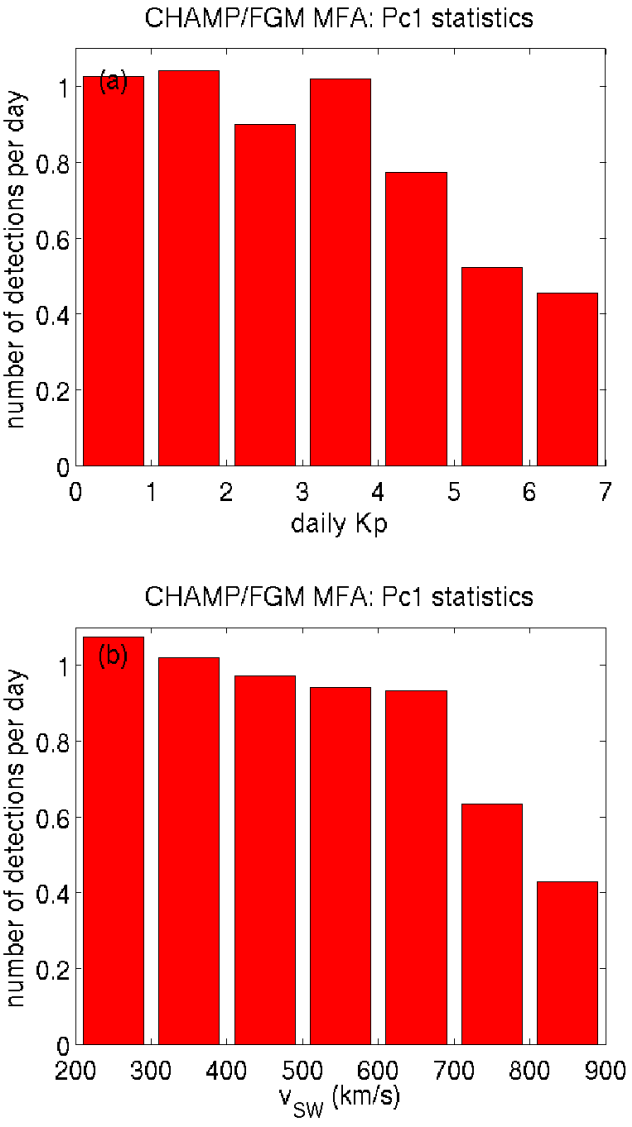

Fig. 9. Dependence of Pc1 occurrence rate on activity as a function **(a)** of Kp index or **(b)** of solar wind velocity.

3.4 Dependence on magnetic activity and solar wind velocity

Figure 9 presents the number of detected Pc1 events per day as a function of magnetic activity (Kp index) and of solar wind velocity. As can be seen from Fig. 9a, the Pc1 event occurrence does not depend much on Kp, but we note a weak preference for less disturbed days (i.e. lower Kp). From Fig. 9b we can deduce that the Pc1 occurrence also exhibits little dependence on solar wind velocity (v_{SW}). The event rates decrease weakly as solar wind velocity increases. Days with solar wind velocities above 900 km s^{-1} will not be considered here because of poor statistics. From these graphs we may conclude that neither high magnetic activity nor strong solar wind input are in favor of Pc1 events.

4 Discussion

With this study we present the first global-scale survey of Pc1 pulsations in the topside ionosphere which covers a full solar cycle. These observations provide insight into a number of Pc1 characteristics. In this section we discuss the properties of the events in comparison with earlier publications.

4.1 Properties of Pc1 pulsation

Many of the features reported here are in line with earlier reports on Pc1. For example our center frequency distribution, shown in Fig. 2a, is consistent with ground observations studied by Bortnik et al. (2007, Fig. 6b) or the results from the ST-5 spacecraft reported by Engebretson et al. (2008, Fig. 9). These authors find center frequencies below 1 Hz for a majority of events. The bandwidth peaking around 0.5 Hz also agrees with Fig. 6e of Bortnik et al. (2007). The narrow bandwidth and moderate spectral amplitude (mostly smaller than 0.5 nT) of our events supports that the Pc1 statistics is not severely contaminated by impulsive magnetic variations or FAC signatures.

It is generally accepted that Pc1 is a manifestation of EMIC waves. Therefore, we may expect Pc1 to exhibit left-handed polarization, at least near the source region, when we consider the rotation sense of the ion cyclotron motion. The linear polarization of our Pc1 events, as shown in Fig. 3a, may be surprising at first sight. However, on their way from the source region to the ionosphere (e.g. near CHAMP altitude) the polarization of the EMIC waves changes significantly: either by an encounter with the cross-over frequency of heavy ions or by superposition of several EMIC wave packets (Denton et al., 1996). In the early-morning MLT sectors, where the Pc1 occurrence rate is maximum in our Fig. 2, Pc1 polarization is generally linear even in the magnetosphere (Anderson et al., 1992b, Fig. 1). Kim et al. (2010, Fig. 8) also presented one morning-side Pc1 event from CHAMP data, which also exhibits linear polarization. All those papers are in general agreement with our Fig. 3.

The dominance of the Pc1 zonal deflections over the meridional amplitudes for ionospheric Pc1 events has never been stated clearly. We again think that this is a consequence of the signal propagation from the magnetospheric source to near-Earth space. From field line resonance theory it is known that zonal oscillations are much less damped than meridional (e.g. Southwood, 1974). Magnetic L shells are largely decoupled when moving in zonal direction, while meridional oscillations always couple energy into the compressional component.

Another property is the duration of Pc1 events, which is in our case of satellite observations equivalent to the latitudinal extent of the wave field (figure not shown). The observed distribution peaks at 30–40 s duration (the minimum period imposed by our detection criterion), which reflects a size of about 2° in latitude. We observe a quasi-exponential decrease of occurrence numbers for longer-lasting events. The e-folding period is about 20 s, which shows that Pc1 events are rather localized events. Due to the orbit geometry of CHAMP we cannot say much about the azimuthal extent of Pc1 events.

4.2 Temporal variation of event rates

The occurrence frequency of Pc1 events exhibits clear climatological features with specific diurnal, annual and solar cycle variations. The MLT dependence is governed by a peak around 04:00 MLT, as shown in our Fig. 4, and a pre-midnight secondary maximum of Pc1 occurrence. This agrees well with Fig. 6c of Bortnik et al. (2007) and with Fig. 10 of Nomura et al. (2011), both of which are based on ground observations at mid-latitudes. Note that these MLT dependences are different from those of higher-latitude ground-based observations (see Kangas et al., 1998, and references therein). The ST-5 observations presented by Engebretson et al. (2008, Fig. 8) are in rough agreement with our results: for $L < 6.6$ (approximately MLAT < 66°) their number of events was larger in the 00:00–10:00 MLT sector than in 10:00–20:00 MLT, but no event was detected in the 20:00–24:00 MLT sector for the same L shells. Erlandson and Anderson (1996) obtained from DE-2 observations a noon-time maximum of Pc1 occurrence (see their Fig. 8), which is not so clear in our Fig. 4a. This difference may be due to the fact that Erlandson and Anderson (1996) used E-field measurements for the Pc1 event detection, while we use B-field fluctuations. Moreover, the local time variation of the DE-2 orbit was locked with the seasonal variation (Saito et al., 1995), which may further contribute to the slight disagreement between our Fig. 4 and Erlandson and Anderson (1996). In our Fig. 4b the center frequency does not exhibit a clear dependence on MLT, which is in general agreement with Fig. 6f of Bortnik et al. (2007).

The seasonal variations, presented in Fig. 5, imply that Pc1 events at CHAMP altitudes favor local summer. Maximum Pc1 occurrence rates are observed around 60° MLAT at nighttime (see Figs. 4 and 7), where the "mid-latitude trough" frequently occurs in the ionospheric F region (Lee et al., 2011, Fig. 3). The trough gets much deeper during local winter: e.g. Lee et al. (2011, Fig. 1) or Xiong et al. (2013, Fig. 2). Hence, we may speculate that a Pc1 encountered by CHAMP favors a high density of local background plasma. On the other hand, previous works using ground-based observations reported that the occurrence rates of mid-latitude Pc1 events are higher in local winter than in summer (e.g. Kuwashima et al., 1981; Nomura et al., 2011). Noting that our Pc1 statistics mainly reflects that of subauroral to mid-latitude regions (see our Fig. 7), this discrepancy appears striking. In order to resolve the discrepancy we have extracted the Pc1 encounters by CHAMP around 110°–180° E GLON, which approximately covers the GLON range of the ground stations used by Nomura et al. (2011, Fig. 1).

Table 1. Harmonic analysis of the Pc1 annual variations, as shown in Fig. 5, separately for the two hemispheres.

	Mean (detection per day)	Annual amplitude (detection per day)	Annual phase (day of the year)	Semi-annual amplitude (detection per day)	Semi-annual phase (day of the year)
Northern Hemisphere	0.44	0.06	237	0.08	31
Southern Hemisphere	0.54	0.15	2	0.10	6

However, the discrepancy (i.e. absence of local winter preference in CHAMP results) persists even in this limited GLON range. Nomura et al. (2011) attributed the local-winter dominance to weak propagation loss in the ionospheric waveguide due to lower F region plasma density. The discrepancy between our results and previous ground-based observations may be due to the influence of the ionospheric E region (e.g. ionospheric screening effect), which acts between ground level and CHAMP altitude. Currently we do not have any good explanation for this discrepancy, and this remains to be resolved by additional coordinated observations.

In Sect. 3.2 we had suggested that the Pc1 occurrence rate is influenced both (1) by the global annual variation of the ionospheric F region with the minimum around the middle of a year (Rishbeth and Müller-Wodarg, 2006) and (2) by the local seasonal variations in the two hemispheres. To investigate this inference more quantitatively we performed harmonic analyses of the data shown in Fig. 5, separately for the two hemispheres. Results of the analysis are listed in Table 1. From the annual mean (the 0th harmonic) we can see that there are about 20 % more events in the Southern Hemisphere. The semi-annual variations (the 2nd harmonic) have much the same amplitudes in the two hemispheres, with a slight bias also toward the Southern Hemisphere. Their phases (day of the year where the maximum occurs) are in rough agreement. Conversely, the annual amplitude (the 1st harmonic) in the Southern Hemisphere is about twice as large compared to the Northern Hemisphere. Let us decompose the annual amplitude in the Southern Hemisphere (0.15) into a global (common for both Northern and Southern Hemispheres) and a local (dependent on hemispheres) component: (1) amplitude of 0.045 for the global annual variation (with the global minimum around June solstice) and (2) amplitude of 0.105 for the local seasonal variation (with the minimum near local winter). Adding these two components in the Southern (Northern) Hemisphere in phase (in anti-phase) roughly leads to the observed total annual amplitude of 0.15 (0.06) as well as the observed annual phase. The semi-annual variations in both hemispheres represent a reduction of Pc1 occurrence rates around equinox seasons.

The solar cycle dependence in Fig. 6 shows that Pc1 events prefer the declining phase of a solar cycle, but the occurrence rates are also high during solar minimum. This is in general agreement with mid-latitude observations by Fraser-Smith (1970). On the other hand, our results are somewhat different from high-latitude observations, for example by Mursula et al. (1991) at Sodankylä ($L \sim 5.1$), where the Pc1 occurrence peaked at solar minimum. Overall, our Pc1 statistic is more in line with the climatology of mid-latitude observations presented in earlier studies: with Fraser-Smith (1970) on the solar cycle dependence, and with Bortnik et al. (2007) and Nomura et al. (2011) on the MLT distributions. Note, however, that solar activity dependence of mid-latitude Pc1 may exhibit differences between different solar cycles. According to Fraser-Smith (1970, Fig. 4) and Guglielmi et al. (2006, Fig. 3) Pc1 activity at a mid-latitude station, Borok ($L \sim 2.9$), is maximum in the declining phase of the 19th solar cycle while the Pc1 activity is nearly anti-correlated with the sunspot number between the 21st and 22nd solar cycle. As our CHAMP data covers only one solar cycle, we cannot investigate differences of Pc1 activity between different solar cycles. This subject is left for future work.

4.3 Spatial distribution of occurrence rate

Our survey shows that Pc1 events are not evenly distributed over the globe. There are distinct latitudes where the detected events tend to cluster. In Fig. 7 we see clear Pc1 occurrence peaks at 55°–60° MLAT. Different from that, magnetospheric observations, e.g. by AMPTE-CCE, reveal significant Pc1 occurrences at even higher L shells (Anderson et al., 1992a, Fig. 12). As outlined in Sect. 2, Pc1 events cannot be detected well at auroral latitudes by LEO satellites because the large-amplitude FAC magnetic fields are masking the Pc1 signatures. This is an inherent limitation of Pc1 studies based on LEO satellite data, such as this or the one by Erlandson and Anderson (1996).

We find only a weak dependence of the Pc1 center frequency on latitude (see Fig. 7) which does not really exceed the range of uncertainty. This finding is at odds with ground-based observations at $L \sim 4.6$ by Sakaguchi et al. (2008, Fig. 10), who reported that the Pc1 frequency increases towards lower latitudes. However, Engebretson et al. (2008, Fig. 9) also found in their ST-5 observations (altitude $= 300 \times 4500$ km) only a marginal correlation between the Pc1 frequency and L shell, although the authors asserted a "general tendency toward higher frequencies at lower L shells". Currently, we don't have a good explanation for this apparent discrepancy between different observations. More coordinated observational studies are needed to give further information on the dependence between the center frequency and latitude.

An actually new result is the geographic distribution of Pc1 events, as shown in Fig. 8. Such a map has never been presented before. We can see that Pc1 events preferentially occur above the Americas, which may imply a connection between the Pc1 generation mechanism and the weak geomagnetic field in the SAA. Considering that Pc1 activity at CHAMP altitudes is higher in summer than in winter, we may speculate that Pc1 in the ionosphere favor (1) weak B-field strength and (2) high background plasma density. One may argue that these two conditions lead to lower Alfvén velocity, which can be expressed by the ratio of E-field over B-field fluctuations (e.g. Saito et al., 1995). However, this interpretation should lead to a larger number of Pc1 events in the SAA than in the northern conjugate region: B-field is weaker (due to the SAA) and plasma density in local summer is higher (Lee et al., 2011, Fig. 1) in the Southern Hemisphere than in the Northern Hemisphere. However, our Fig. 8b shows that the occurrence rate peak is larger in the Northern Hemisphere than in the Southern Hemisphere. More theoretical studies and simulations are needed to clarify the relationship between local Alfvén velocity and strength of Pc1 magnetic signatures.

Generally, there are only a few Pc1 events detected poleward of 65° MLAT. We have checked these events carefully to make sure that they are not false detections. This subgroup of auroral latitude Pc1 events reveals quite special characteristics (figures not shown). The MLT distribution clearly peaks around noon with sizable occurrence rates confined to the 08:00–14:00 MLT sector. This result is in line with magnetospheric observations by Anderson et al. (1992a) on L shells beyond 7. It is just this subgroup that is responsible for the minor peak at noon in Fig. 4a. Since this subgroup is under-represented in the total statistics (due to the above-mentioned limitations of LEO observations), the noon occurrence peak may be larger in reality (i.e. near the magnetospheric source region). The center frequency of the auroral zone events is mostly below 1 Hz. All the other properties, like ellipticity, orientation of major axis, bandwidth, etc., are in general consistency with those in our Figs. 2–3. The yearly Pc1 occurrence poleward of 65° MLAT exhibits a maximum in 2009, which is much later than in Fig. 6. This result is consistent with the Pc1 statistics at an auroral-latitude observatory, Sodankylä (Finland) (Mursula et al., 1991). A majority of these high-latitude events were detected at low magnetic activity and slow solar wind. Under those conditions FACs are expected to be weak, which may otherwise mask Pc1 events at auroral latitudes from CHAMP observations.

4.4 Dependence on magnetic activity and solar wind velocity

According to previous papers Pc1 occurrence does not depend much on magnetic activity. For example, isolated proton arcs, which often accompany Pc1 events, occur under any geomagnetic conditions (Sakaguchi et al., 2008). Actually, their Fig. 4 implies that isolated proton arcs avoid severely disturbed period around storm-time Dst minima. This is largely consistent with our results (see Fig. 9a). The slight preference for quiet conditions may also be the reason for reduced Pc1 occurrence rates during equinox seasons (see Fig. 5), when magnetic activity is known to be enhanced (Russell and McPherron, 1973). However, Pc1 pulsations can be categorized into several subclasses, such as the pearl type or the intervals of pulsations of diminishing periods (IPDP). Readers should note that the subclass occurrence rates may depend on Kp in a way different from that of our Fig. 9a. For example, Kangas et al. (1998, Fig. 10) shows that more IPDP events were observed at the Sodankylä observatory ($L \sim 5.1$) for $\mathrm{Kp} \geq 3$ than for $\mathrm{Kp} < 3$. Our detection method cannot discriminate between subclasses of Pc1 pulsations, and is not suitable for detecting Pc1 pulsations at auroral latitudes, e.g. near the Sodankylä observatory. Therefore, we cannot give a definitive answer as to the dependence of Pc1 subclasses on Kp. Observational studies using a global network of ground observatories would help to solve this problem.

The Pc1 occurrence maximum appeared around 2004–2005 (Fig. 6), when recurrent solar wind streams were quite active. In that context the weak negative correlation between Pc1 occurrence and solar wind velocity is quite unexpected (see Fig. 9b). However, our results are consistent with Guglielmi et al. (2005), who also reported that slow solar wind creates a favorable condition for pearl-type Pc1 events observed at the Sodankylä observatory ($L \sim 5.1$). It seems that fast solar wind velocity events cannot be a prime driver of Pc1. Rather, instabilities internal to the terrestrial plasma system may play a significant role in Pc1 generations. For example, spontaneous instabilities near the bow shock, which drive among others traveling convection vortices, may be related to Pc1 generations (Engebretson et al., 2013). More and coordinated studies including multi-point observations are needed to disentangle the processes causing Pc1 events.

5 Summary

This study presents a survey of Pc1 pulsations detected in magnetic field observations by the CHAMP satellite over the period 2000 to 2010. We have compiled a list of 3616 Pc1 events detected by CHAMP. The long-term observations with quasi-continuous temporal and global coverage have enabled us to reveal a Pc1 climatology at LEO altitudes more complete than ever. A limitation of the survey is that Pc1 events cannot be detected in regions of strong field-aligned current activity, e.g. within the auroral zone. From our statistical analysis we draw the following conclusions.

1. *Wave properties*: The Pc1 center frequency varies around 1 Hz, and the bandwidth is on average 0.5 Hz. Both results agree well with previous works. The observed wave signal is highly polarized within the plane

perpendicular to the main field, and the ellipticity is generally linear with the major axis aligned within 15° from the zonal direction. Spectral amplitudes of Pc1 pulsations are small (mostly around 0.2 nT).

2. *Temporal variations*: The diurnal variation of Pc1 occurrences exhibits an early-morning peak and a secondary maximum at pre-midnight hours. Both of these results agree well with previous ground-based observations at mid-latitudes. The annual variations of occurrence rates are quite different in the two hemispheres, with a preference of the local summer season. Reduced Pc1 occurrences are observed around equinoxes. Superimposed on the seasonal variation is a small influence of the global annual cycle of the ionosphere with a minimum near June. The solar cycle dependence reveals a clear peak of Pc1 occurrence rates at the declining phase (2004–2005). In general, occurrence rates are significantly higher during solar minimum years than during maximum years.

3. *Dependence on magnetic activity and solar wind velocity*: We find a weakly negative dependence of Pc1 occurrence rate on magnetic activity for quiet and moderately disturbed times ($Kp \leq 6.3$). The same is valid for solar wind velocity ($v_{SW} < 900\,km\,s^{-1}$). Other factors than Kp or v_{SW} seem to contribute significantly to the generation of Pc1 pulsations.

4. *Latitudinal variations I*: Our survey shows a Pc1 occurrence peak at 55°–60° MLAT. The steep cutoff towards higher latitudes is caused by the large-amplitude FAC signatures masking the Pc1 pulsations. For the center frequency of Pc1 pulsations we do not find a significant increase/decrease with latitude. This result is at odds with previous ground-based observations, but generally consistent with ST-5 satellite observations.

5. *Latitudinal variations II*: Pc1 events are occasionally detected at auroral latitudes, where Pc1 events are usually masked by strong FAC. This subset of high-latitude events shows a clear occurrence peak around noon and near solar minimum. This result is different from the bulk of our subauroral events, but is consistent with Pc1 observations in the outer magnetosphere.

6. *Longitudinal variations*: The global distribution of Pc1 exhibits highest occurrence rates over the Americas. This sector coincides with the longitudes of the SAA. Pc1 driving mechanisms seem to favor this region of small geomagnetic field strengths.

The average properties of Pc1 events outlined here provide a valuable frame for interpreting previous observations in a global context. For further investigations we plan to make use of our event catalogue to perform, for example, conjugate event studies with ground-based and/or magnetospheric observations. Furthermore, we plan to study the generation mechanisms with the help of superposed epoch analyses related to storms, substorms and other possible geophysical drivers.

Acknowledgements. The authors gratefully acknowledge valuable discussions with T. Iyemori and C. Stolle. The CHAMP mission was sponsored by the Space Agency of the German Aerospace Center (DLR) through funds of the Federal Ministry of Economics and Technology, following a decision of the German Federal Parliament (grant code 50EE0944).

The service charges for this open access publication have been covered by a Research Centre of the Helmholtz Association.

Topical Editor L. Blomberg thanks two anonymous referees for their help in evaluating this paper.

References

Anderson, B. J. and Fuselier, S. A.: Magnetic pulsations from 0.1 to 4.0 Hz and associated plasma properties in the Earth's subsolar magnetosheath and plasma depletion layer, J. Geophys. Res., 98, 1461–1479, 1993.

Anderson, B. J., Fuselier, S. A., and Murr, D.: Electromagnetic ion cyclotron waves observed in the plasma depletion layer, Geophys. Res. Lett., 18, 1955–1958, 1991.

Anderson, B. J., Erlandson, R. E., and Zanetti, L. J.: A statistical study of Pc 1–2 magnetic pulsations in the equatorial magnetosphere: 1. Equatorial occurrence distributions, J. Geophys. Res., 97, 3075–3088, doi:10.1029/91JA02706, 1992a.

Anderson, B. J., Erlandson, R. E., and Zanetti, L. J.: A statistical study of Pc 1–2 magnetic pulsations in the equatorial magnetosphere: 2. Wave properties, J. Geophys. Res., 97, 3089–3101, doi:10.1029/91JA02697, 1992b.

Anderson, B. J., Erlandson, R. E., Engebretson, M. J., Alford, J. L., and Arnoldy, R. L.: Source region of 0.2 to 1.0 Hz geomagnetic pulsation bursts, Geophys. Res. Lett., 23, 769–772, 1996.

Bortnik, J., Cutler, J. W., Dunson, C., and Bleier, T. E.: An automatic wave detection algorithm applied to Pc1 pulsations, J. Geophys. Res., 112, A04204, doi:10.1029/2006JA011900, 2007.

Bräysy, T., Mursula, K., and Marklund, G.: Ion cyclotron waves during a great magnetic storm observed by Freja double-probe electric field instrument, J. Geophys. Res., 103, 4145–4155, doi:10.1029/97JA02820, 1998.

Clausen, L. B. N., Baker, J. B. H., Ruohoniemi, J. M., and Singer, H. J.: EMIC waves observed at geosynchronous orbit during solar minimum: Statistics and excitation, J. Geophys. Res., 116, A10205, doi:10.1029/2011JA016823, 2011.

Denton, R. E., Anderson, B. J., Ho, G., and Hamilton, D. C.: Effects of wave superposition on the polarization of electromagnetic ion cyclotron waves, J. Geophys. Res., 101, 24869–24885, doi:10.1029/96JA02251, 1996.

Engebretson, M. J., Posch, J. L., Westerman, A. M., Otto, N. J., Slavin, J. A., Le, G., Strangeway, R. J., and Lessard, M. R.: Temporal and spatial characteristics of Pc1 waves observed by ST5, J. Geophys. Res., 113, A07206, doi:10.1029/2008JA013145, 2008.

Engebretson, M. J., Moen, J., Posch, J. L., Lu, F., Lessard, M. R., Kim, H., and Lorentzen, D. A.: Searching for ULF signatures of the cusp: Observations from search coil magnetometers and

auroral imagers in Svalbard, J. Geophys. Res., 114, A06217, doi:10.1029/2009JA014278, 2009.

Engebretson, M. J., Kahlstorf, C. R. G., Murr, D. L., Posch, J. L., Keiling, A., Lavraud, B., Rème, H., Lessard, M. R., Kim, E.-H., Johnson, J. R., Dombeck, J., Grison, B., Robert, P., Glassmeier, K.-H., and Décréau, P. M. E.: Cluster observations of band-limited Pc 1 waves associated with streaming H^+ and O^+ ions in the high-altitude plasma mantle, J. Geophys. Res., 117, A10219, doi:10.1029/2012JA017982, 2012.

Engebretson, M. J., Yeoman, T. K., Oksavik, K., Søraas, F., Sigernes, F., Moen, J. I., Johnsen, M. G., Pilipenko, V. A., Posch, J. L., Lessard, M. R., Lavraud, B., Hartinger, M. D., Clausen, L. B. N., Raita, T., and Stolle, C.: Multi-instrument observations from Svalbard of a traveling convection vortex, electromagnetic ion cyclotron wave burst, and proton precipitation associated with a bow shock instability, J. Geophys. Res. Space Physics, 118, 2975–2997, doi:10.1002/jgra.50291, 2013.

Erlandson, R. E., Zanetti, L. J., Potemra, T. A., Block, L. P., and Holmgren, G.: Viking magnetic and electric field observations of Pc 1 waves at high latitudes, J. Geophys. Res., 95, 5941–5955, doi:10.1029/JA095iA05p05941, 1990.

Erlandson, R. E. and Anderson, B. J.: Pc 1 waves in the ionosphere: A statistical study, J. Geophys. Res., 101, 7843–7857, doi:10.1029/96JA00082, 1996.

Erlandson, R. E. and Ukhorskiy, A. J.: Observations of electromagnetic ion cyclotron waves during geomagnetic storms: Wave occurrence and pitch angle scattering, J. Geophys. Res., 106, 3883–3895, doi:10.1029/2000JA000083, 2001.

Fowler, R. A., Kotick, B. J., and Elliott, R. D.: Polarization analysis of natural and artificially induced geomagnetic micropulsations, J. Geophys. Res., 72, 2871–2883, doi:10.1029/JZ072i011p02871, 1967.

Fraser, B. J., Singer, H. J., Hughes, W. J., Wygant, J. R., Anderson, R. R., and Hu, Y. D.: CRRES Poynting vector observations of electromagnetic ion cyclotron waves near the plasmapause, J. Geophys. Res., 101, 15331–15343, doi:10.1029/95JA03480, 1996.

Fraser-Smith, A. C.: Some statistics on Pc 1 geomagnetic micropulsation occurrence at middle latitudes: Inverse relation with sunspot cycle and semi-annual period, J. Geophys. Res., 75, 4735–4745, doi:10.1029/JA075i025p04735, 1970.

Guglielmi, A. and Kangas, J.: Pc1 waves in the system of solar–terrestrial relations: New reflections, J. Atmos. Solar-Terr. Phys., 69, 1635–1643, doi:10.1016/j.jastp.2007.01.015, 2007.

Guglielmi, A. and Pokhotelov, O.: Geoelectromagnetic Waves, IOP Publ. Ltd. Bristol and Philadelphia, 1996.

Guglielmi, A., Kangas, J., Kultima, J., and Potapov, A.: Solar wind dependence of the Pc1 wave activity, Adv. Space Res., 36, 2413–2416, 2005.

Guglielmi, A., Potapov, A., Matveyeva, E., Polyushkina, T., and Kangas, J.: Temporal and spatial characteristics of Pc1 geomagnetic pulsations, Adv. Space Res., 38, 1572–1575, 2006.

Halford, A. J., Fraser, B. J., and Morley, S. K.: EMIC wave activity during geomagnetic storm and nonstorm periods: CRRES results, J. Geophys. Res., 115, A12248, doi:10.1029/2010JA015716, 2010.

Iyemori, T. and Hayashi, K.: PC 1 micropulsations observed by Magsat in the ionospheric F region, J. Geophys. Res., 94, 93–100, doi:10.1029/JA094iA01p00093, 1989.

Iyemori, T., Sugiura, M., Oka, A., Morita, Y., Ishii, M., Slavin, J. A., Brace, L. H., Hoffman, R. A., and Winningham, J. D.: Localized injection of large-amplitude Pc 1 waves and electron temperature enhancement near the plasmapause observed by DE 2 in the upper ionosphere, J. Geophys. Res., 99, 6187–6199, doi:10.1029/93JA02750, 1994.

Kangas, J., Guglielmi, A., and Pokhotelov, O.: Morphology and physics of short-period magnetic pulsations, Space Sci. Rev., 83, 435–512, 1998.

Kawamura, M., Kuwashima, M., Toya, T., and Fukunishi, H.: Comparative study of magnetic pc 1 pulsations observed at low and high latitudes: Long-term variation of occurrence frequency of the pulsations, National Institute Polar Research Memoirs, 26, 1–12, March 1983.

Keika, K., Takahashi, K., Ukhorskiy, A. Y., and Miyoshi, Y.: Global characteristics of electromagnetic ion cyclotron waves: Occurrence rate and its storm dependence, J. Geophys. Res. Space Physics, 118, 4135–4150, doi:10.1002/jgra.50385, 2013.

Kim, H., Lessard, M. R., Engebretson, M. J., and Lühr, H.: Ducting characteristics of Pc 1 waves at high latitudes on the ground and in space, J. Geophys. Res., 115, A09310, doi:10.1029/2010JA015323, 2010.

Kim, H., Lessard, M. R., Engebretson, M. J., and Young, M. A.: Statistical study of Pc1-2 wave propagation characteristics in the high-latitude ionospheric waveguide, J. Geophys. Res., 116, A07227, doi:10.1029/2010JA016355, 2011.

Kuwashima, M., Toya, T., Kawamura, M., Hirasawa, T., Fukunishi, H., and Ayukawa, M.: Comparative Study of Magnetic Pc1 Pulsations between Low Latitudes and High Latitudes: Statistical Study, National Institute Polar Research Memoirs, 18, 101–117, March 1981.

Lee, I. T., Wang, W., Liu, J. Y., Chen, C. Y., and Lin, C. H.: The ionospheric midlatitude trough observed by FORMOSAT-3/COSMIC during solar minimum, J. Geophys. Res., 116, A06311, doi:10.1029/2010JA015544, 2011.

Lysak, R. L. and Yoshikawa, A.: Resonant Cavities and Waveguides in the Ionosphere and Atmosphere, in: Magnetospheric ULF Waves: Synthesis and New Directions, edited by: Takahashi, K., Chi, P. J., Denton, R. E., and Lysak, R. L., American Geophysical Union, Washington, D.C., doi:10.1029/169GM19, 2006.

Lysak, R. L., Waters, C. L., and Sciffer, M. D.: Modeling of the ionospheric Alfvén resonator in dipolar geometry, J. Geophys. Res. Space Physics, 118, 1514–1528, doi:10.1002/jgra.50090, 2013.

Min, K., Lee, J., Keika, K., and Li, W.: Global distribution of EMIC waves derived from THEMIS observations, J. Geophys. Res., 117, A05219, doi:10.1029/2012JA017515, 2012.

Miyoshi, Y., Sakaguchi, K., Shiokawa, K., Evans, D., Albert, J., Connors, M., and Jordanova, V.: Precipitation of radiation belt electrons by EMIC waves, observed from ground and space, Geophys. Res. Lett., 35, L23101, doi:10.1029/2008GL035727, 2008.

Mursula, K.: Satellite observations of Pc 1 pearl waves: The changing paradigm, J. Atmos. Solar Terr. Phys., 69, 1623–1634, doi:10.1016/j.jastp.2007.02.013, 2007.

Mursula, K., Kangas, J., Pikkarainen, T., and Kivinen, M.: Pc 1 micropulsations at a high-latitude station: A study over nearly four solar cycles, J. Geophys. Res., 96, 17651–17661,

doi:10.1029/91JA01374, 1991.

Mursula, K., Bräysy, T., Niskala, K., and Russell, C. T.: Pc1 pearls revisited: Structured electromagnetic ion cyclotron waves on Polar satellite and on ground, J. Geophys. Res., 106, 29543–29553, doi:10.1029/2000JA003044, 2001.

Nomura, R., Shiokawa, K., Pilipenko, V., and Shevtsov, B.: Frequency-dependent polarization characteristics of pc1 geomagnetic pulsations observed by multi-point ground stations at low latitudes, J. Geophys. Res., 116, A01204, doi:10.1029/2010JA015684, 2011.

Nomura, R., Shiokawa, K., Sakaguchi, K., Otsuka, Y., and Connors, M.: Polarization of Pc1/EMIC waves and related proton auroras observed at subauroral latitudes, J. Geophys. Res., 117, A02318, doi:10.1029/2011JA017241, 2012.

Park, J., Lühr, H., Stolle, C., Rother, M., Min, K. W., Chung, J.-K., Kim, Y. H., Michaelis, I., and Noja, M.: Magnetic signatures of medium-scale traveling ionospheric disturbances as observed by CHAMP, J. Geophys. Res., 114, A03307, doi:10.1029/2008JA013792, 2009.

Posch, J. L., Engebretson, M. J., Murphy, M. T., Denton, M. H., Lessard, M. R., and Horne, R. B.: Probing the relationship between electromagnetic ion cyclotron waves and plasmaspheric plumes near geosynchronous orbit, J. Geophys. Res., 115, A11205, doi:10.1029/2010JA015446, 2010.

Rishbeth, H. and Müller-Wodarg, I. C. F.: Why is there more ionosphere in January than in July? The annual asymmetry in the F2-layer, Ann. Geophys., 24, 3293–3311, doi:10.5194/angeo-24-3293-2006, 2006.

Roldugin, V. C., Roldugin, A. V., and Pilgaev, S. V.: Pc1–2 auroral pulsations, J. Geophys. Res. Space Physics, 118, 74–81, doi:10.1029/2012JA017861, 2013.

Rother, M., Schlegel, K., and Lühr, H.: CHAMP observation of intense kilometer-scale field-aligned currents, evidence for an ionospheric Alfvén resonator, Ann. Geophys., 25, 1603–1615, doi:10.5194/angeo-25-1603-2007, 2007.

Russell, C. T. and McPherron, R. L.: Semiannual variation of geomagnetic activity, J. Geophys. Res., 78, 92–108, 1973.

Safargaleev, V., Serebryanskaya, A., Koustov, A., Lester, M., Pchelkina, E., and Vasilyev, A.: A possible origin of dayside Pc1 magnetic pulsations observed at high latitudes, Ann. Geophys., 22, 2997–3008, doi:10.5194/angeo-22-2997-2004, 2004.

Saito, A., Iyemori, T., Sugiura, M., Maynard, N. C., Aggson, T. L., Brace, L. H., Takeda, M., and Yamamoto, M.: Conjugate occurrence of the electric field fluctuations in the nighttime midlatitude ionosphere, J. Geophys. Res., 100, 21439–21451, doi:10.1029/95JA01505, 1995.

Sakaguchi, K., Shiokawa, K., Miyoshi, Y., Otsuka, Y., Ogawa, T., Asamura, K., and Connors, M.: Simultaneous appearance of isolated auroral arcs and Pc 1 geomagnetic pulsations at subauroral latitudes, J. Geophys. Res., 113, A05201, doi:10.1029/2007JA012888, 2008.

Southwood, D. J.: Some features of field line resonances in the magnetosphere, Planet. Space Sci., 22, 483–491, 1974.

Stolle, C., Lühr, H., Rother, M., and Balasis, G.: Magnetic signatures of equatorial spread F as observed by the CHAMP satellite, J. Geophys. Res., 111, A02304, doi:10.1029/2005JA011184, 2006.

Xiong, C., Lühr, H., and Ma, S. Y.: The subauroral electron density trough: Comparison between satellite observations and IRI-2007 model estimates, Adv. Space Res., 51, 536–544, doi:10.1016/j.asr.2011.09.021, 2013.

Yahnin, A. G., Yahnina, T. A., Frey, H. U., Bösinger, T., and Manninen, J.: Proton aurora related to intervals of pulsations of diminishing periods, J. Geophys. Res., 114, A12215, doi:10.1029/2009JA014670, 2009.